Vibronic analysis of fluorescence spectrum of NO2 D 2 B 2(0,0,0) in the region of 250–550 nm

Kaoru Aoki, Kennosuke Hoshina, and Kazuhiko Shibuya

Citation: The Journal of Chemical Physics **105**, 2228 (1996); doi: 10.1063/1.472117
View online: http://dx.doi.org/10.1063/1.472117
View Table of Contents: http://scitation.aip.org/content/aip/journal/jcp/105/6?ver=pdfcov
Published by the AIP Publishing

Vibronic analysis of fluorescence spectrum of NO_2 $\tilde{D}\,^2B_2(0,0,0)$ in the region of 250–550 nm

Kaoru Aoki,[a] Ken-nosuke Hoshina, and Kazuhiko Shibuya
Department of Chemistry, Tokyo Institute of Technology, 2-12-1 Ohokayama, Meguro-ku, Tokyo 152, Japan

(Received 15 March 1996; accepted 25 April 1996)

The dispersed fluorescence spectrum of NO_2 $\tilde{D}\,^2B_2(0,0,0)$ was measured and analyzed in the spectral range of 250–550 nm. The strong fluorescence bands in 250–350 nm correspond to $\tilde{D}\,^2B_2(0,0,0)\rightarrow\tilde{X}\,^2A_1(n_1=0\text{–}9,\ n_2=0\text{–}5,\ n_3=0)$ with a Franck–Condon maximum at $n_1=4$ and $n_2=0$. The weak and broad bands in 350–410 nm are built on a progression of bending frequency, 710 cm^{-1}. The lower state responsible for this fluorescence was interpreted as admixture $^{ev}B_2$ levels generated by a vibronic coupling between a_1-vibrational levels on $\tilde{A}\,^2B_2$ and highly excited b_2 levels on $\tilde{X}\,^2A_1$. The medium-intensity bands in 410–550 nm were assigned to $\tilde{D}\,^2B_2(0,0,0)\rightarrow\tilde{C}\,^2A_2(n_1=0\text{–}2,\ n_2=0\text{–}5,\ n_3=0\text{–}2)$ with a Franck–Condon maximum at $n_1=0$, $n_2=2$, and $n_3=0$. The vibrational frequencies of $\tilde{C}\,^2A_2$ are 1010 cm^{-1} for symmetric stretch (ω_1), 740 cm^{-1} for bending (ω_2), and 250 cm^{-1} for antisymmetric stretch (ω_3). The simple Franck–Condon calculation for $\tilde{D}\,^2B_2(0,0,0)\rightarrow\tilde{C}\,^2A_2(n_1,n_2,n_3)$ gives the approximate geometry of the $\tilde{C}\,^2A_2$ state as r(N–O)$\sim$134 pm and $\theta\sim$108°. The partial rotational structure of $\tilde{C}\,^2A_2(0,0,0)$ was analyzed using an optical–optical double resonance measurement, which confirms the A_2 vibronic symmetry. The origin of NO_2 $\tilde{C}\,^2A_2$ (T_0) was determined to be around 16 234 cm^{-1}. © *1996 American Institute of Physics.* [S0021-9606(96)01929-0]

I. INTRODUCTION

Nitrogen dioxide in a $\tilde{C}\,^2A_2$ state cannot be prepared directly by the photoexcitation of NO_2 in the ground state ($\tilde{X}\,^2A_1$), because the A_1–A_2 transition is symmetry forbidden. Information on NO_2 $\tilde{C}\,^2A_2$ has not been experimentally obtained until recently. In 1989, the first observation of the $\tilde{C}\,^2A_2$ state was reported by Weaver *et al.*[1] using the photoelectron spectroscopy of NO_2^-. NO_2 $\tilde{C}\,^2A_2$ is accessible via one-electron photodetachment from NO_2^- $\tilde{X}\,^1A_1$, and they reported the band origin (T_0) of $\tilde{C}\,^2A_2$ to be 2.028±0.009 eV (16 360±70 cm^{-1}) from the vibronic structure of the photoelectron spectra.

We have confirmed the contribution of $\tilde{C}\,^2A_2$ to the visible absorption spectrum of NO_2 by applying an optical–optical double resonance (OODR) method.[2–4] In the 514–590 nm region of the visible absorption system, we have observed a number of rovibronic levels yielded by the spin–orbit interaction between $\tilde{C}\,^2A_2$ and $^{ev}B_2$ states. Here, $^{ev}B_2$ denotes admixtures of the a_1-vibrational levels on $\tilde{A}\,^2B_2$ and the b_2-vibrational levels on $\tilde{X}\,^2A_1$. In the OODR excitation using two visible laser lights, the first and second steps are assigned to $^{ev}B_2\leftarrow\tilde{X}\,^2A_1(0,0,0)$ and $\tilde{D}\,^2B_2(0,0,0)\leftarrow{}^{ev}A_2$, respectively. This OODR excitation mechanism suggests that the dispersed fluorescence (DF) spectrum of NO_2 $\tilde{D}\,^2B_2$ in the visible region will provide the vibronic information on $\tilde{C}\,^2A_2$.

The DF spectrum of NO_2 $\tilde{D}\,^2B_2$ was first measured by Tsukiyama *et al.*[5] They tentatively assigned the visible fluorescence bands to $\tilde{D}\,^2B_2(0,0,0)\rightarrow\tilde{A}\,^2B_2(n_1,n_2,n_3)$ for the following reasons. (1) The lower levels responsible for the visible fluorescence of $\tilde{D}\,^2B_2$, lying around 2 eV above the ground state, could be prepared by the visible light absorption of NO_2 $\tilde{X}\,^2A_1$. (2) The oscillator strength of the visible absorption is well-known to be carried mainly by $\tilde{A}\,^2B_2$–$\tilde{X}\,^2A_1$ and additionally by $\tilde{B}\,^2B_1$–$\tilde{X}\,^2A_1$. It was not known at that time that a symmetry-forbidden $\tilde{C}\,^2A_2$–$\tilde{X}\,^2A_1$ transition contributes to the visible absorption system. (3) The $\tilde{D}\,^2B_2$–$\tilde{A}\,^2B_2$ transition is symmetry allowed, while the $\tilde{D}\,^2B_2$–$\tilde{B}\,^2B_1$ transition is symmetry forbidden.

The fluorescence intensity of $\tilde{D}\,^2B_2$ is extremely weak due to its predissociative character: The minimum predissociation linewidth of $\tilde{D}\,^2B_2$ is 0.1 cm^{-1}, corresponding to the lifetime of 42 ps, at the zero vibrational level.[6] In the present study, we have improved the signal-to-noise (S/N) ratio and spectral resolution of the DF spectrum of NO_2 $\tilde{D}\,^2B_2$ and measured the spectrum in 250–550 nm. The detailed analysis has been made after classifying the DF spectrum into three spectral regions—250–350 nm, 350–410 nm, and 410–550 nm. The 250–350 nm fluorescence corresponds to $\tilde{D}\,^2B_2(0,0,0)\rightarrow\tilde{X}\,^2A_1(n_1,n_2,n_3)$. The weak bands in 350–410 nm present a progression characterized by the bending frequency (710 cm^{-1}) of $\tilde{A}\,^2B_2$. These bands are assigned to $\tilde{D}\,^2B_2(0,0,0)\rightarrow{}^{ev}B_2$, where $^{ev}B_2$ is the admixture state with $^{ev}B_2$ symmetry yielded by strong vibronic coupling between $\tilde{X}\,^2A_1$ and $\tilde{A}\,^2B_2$. The 410–550 nm bands are newly assigned to $\tilde{D}\,^2B_2(0,0,0)\rightarrow\tilde{C}\,^2A_2(n_1,n_2,n_3)$. The origin ($T_0$), vibrational frequencies (ω_1, ω_2, and ω_3), and geometry [r(N–O) and θ] of the $\tilde{C}\,^2A_2$ state are reported for the first

[a]Present address: Yonago National College of Technology, 4448 Hikona, Tottori 683, Japan.

time. The partial rotational structure of $\tilde{C}\ ^2A_2(0,0,0)$ is analyzed using an OODR measurement.

II. EXPERIMENT

A. Dispersed fluorescence measurement

The frequency-doubled output (around 249.29 nm) of a dye laser (Lumonics HD 300) pumped by the third harmonics of a Nd:YAG laser (Lumonics HY750) was used to excite NO_2 from $\tilde{X}\ ^2A_1(0,0,0)$ to $\tilde{D}\ ^2B_2(0,0,0)$. The DF spectrum was measured using a monochromator (Nikon P250) with a grating of 1200 grooves mm^{-1} blazed at 300 or 500 nm and a photomultiplier (Hamamatsu R928 or 1P28). The photomultiplier signals were averaged by a boxcar integrator (Stanford Research Systems SR250) and stored on a personal computer. The wavelength calibration of the monochromator was made by atomic lines of a mercury lamp. The spectral sensitivity of the detection system in the visible region was calibrated using the emission of 3 ml/ℓ quinoline–ethanol solution excited at 303 nm.[7] The sample pressure was kept about 10 Torr at room temperature. Under this pressure condition, the fluorescence intensity of NO_2 $\tilde{D}\ ^2B_2(0,0,0)$ was maximized enough to measure the vibronically resolved spectrum. The collisional relaxation of $\tilde{D}\ ^2B_2(0,0,0)$ can be ignored, because it is predissociative and short-lived (42 ps).[6]

B. Optical–optical double resonance measurement

The experimental details have been described elsewhere.[8] The output beam of a XeCl excimer laser (Lambda Physik EMG-103E MSC) was split into two beams to simultaneously excite pump and probe dye lasers (Lambda Physik FL-2002E). The frequency of the first pump laser with an etalon (ν_1, the bandwidth of 0.04 cm^{-1}) was tuned to a rovibronic band in the visible absorption of NO_2, while the second probe laser (ν_2, 0.3 cm^{-1} without an etalon) was used further to excite NO_2 to $\tilde{D}\ ^2B_2$. The delay between two dye laser pulses was about 10 ns throughout the present experiments. The frequency calibration of the pump and probe lasers was made by the laser-induced fluorescence spectrum of I_2 and the optogalvanic spectrum of Ne, respectively. The occurrence of the double resonance was monitored by observing the UV fluorescence corresponding to the radiative $\tilde{D}\rightarrow\tilde{X}$ transition. The fluorescence was detected by a solar-blind photomultiplier (Hamamatsu R166) through aqueous solution of $NiSO_4/CoSO_4$ and a bandpass filter (Corning 7-54). The photomultiplier signals were recorded by a boxcar integrator (PAR162/165) after being amplified by a preamplifier (PAR 115). The sample pressure was kept about 1 Torr to avoid collisional relaxation of ν_1-excited intermediate levels.

Two kinds of OODR excitation spectra were measured for an intermediate single rovibronic level. A ν_2-scanned spectrum was obtained by fixing ν_1, which reflects the rotational structure of the final $\tilde{D}\ ^2B_2(0,0,0)$. Alternatively, a ν_1-scanned spectrum measured by fixing ν_2 reflects the rotational structure of the initial $\tilde{X}\ ^2A_1(0,0,0)$. The conclusive rotational assignment of the intermediate level can be obtained independently from the two spectra. The rotational energies of intermediate levels were calculated using the spectroscopic constants reported on $\tilde{X}\ ^2A_1(0,0,0)$[9] and $\tilde{D}\ ^2B_2(0,0,0)$,[6] and the ν_1- and ν_2-transition energies determined by the OODR excitation spectra.

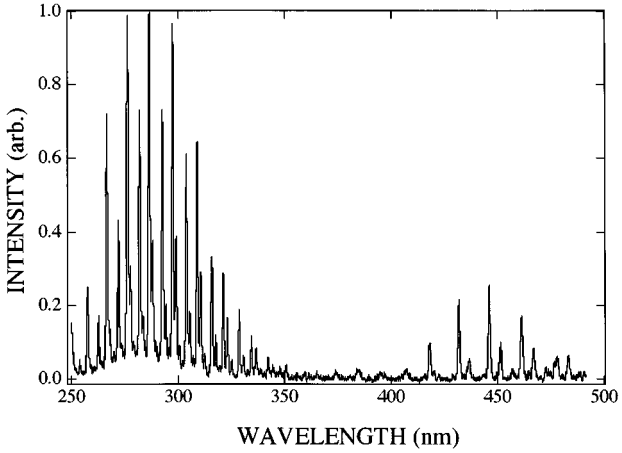

FIG. 1. Overview of dispersed fluorescence (DF) spectrum of NO_2 $\tilde{D}\ ^2B_2(0,0,0)$. The NO_2 molecule was excited with the laser light at 249.29 nm near the $^qR_2$ bandhead of $\tilde{D}\ ^2B_2(0,0,0)\leftarrow\tilde{X}\ ^2A_1(0,0,0)$.

III. DISPERSED FLUORESCENCE

Figure 1 shows the DF spectrum of NO_2 $\tilde{D}\ ^2B_2(0,0,0)$, where NO_2 was excited with UV light at 249.29 nm near the $^qR_2$ bandhead of $\tilde{D}\ ^2B_2(0,0,0)-\tilde{X}\ ^2A_1(0,0,0)$. The DF spectrum of the $\tilde{D}$ state was first measured by Tsukiyama *et al.*,[5] although the S/N ratio was rather low at that time. They found two band systems in the UV and visible regions and assigned them to $\tilde{D}\ ^2B_2-\tilde{X}\ ^2A_1$ and $\tilde{D}\ ^2B_2-\tilde{A}\ ^2B_2$, respectively. In the present study, the S/N ratio was much improved and another weak band system in the region of 350–410 nm was newly observed. The DF spectrum is vibronically analyzed by classifying it into three spectral regions—250–350 nm, 350–410 nm, and 410–550 nm.

A. $\tilde{D}\ ^2B_2(0,0,0)\rightarrow\tilde{X}\ ^2A_1(n_1,n_2,n_3)$ transition

Figure 2(a) shows the DF spectrum in the UV region, which is assigned to NO_2 $\tilde{D}\ ^2B_2(0,0,0)\rightarrow\tilde{X}\ ^2A_1(n_1,n_2,n_3)$. The vibrational term values of $\tilde{X}\ ^2A_1$ are well fitted using the Dunham parameters determined by Delon and Jost.[10] They analyzed the visible DF spectrum of NO_2 $^{ev}B_2$ excited with the visible light, and the 191 vibrational levels on $\tilde{X}\ ^2A_1$ are fitted with the Dunham expansion. The fluorescence bands in 250–350 nm are thus assigned to $\tilde{D}\ ^2B_2(0,0,0)\rightarrow\tilde{X}\ ^2A_1(n_1=0\text{–}9,\ n_2=0\text{–}5,\ n_3=0)$ with a Franck–Condon maximum at $n_1=4$ and $n_2=0$.

The equilibrium geometry of $\tilde{D}\ ^2B_2(0,0,0)$ was obtained to be $r(\text{N–O})=131.4$ pm and $\theta=120.9°$ from the rotational analysis of the $\tilde{D}\ ^2B_2(0,0,0)\leftarrow\tilde{X}\ ^2A_1(0,0,0)$ absorption.[6] The vibrational frequencies of $\tilde{D}\ ^2B_2$ were reported as

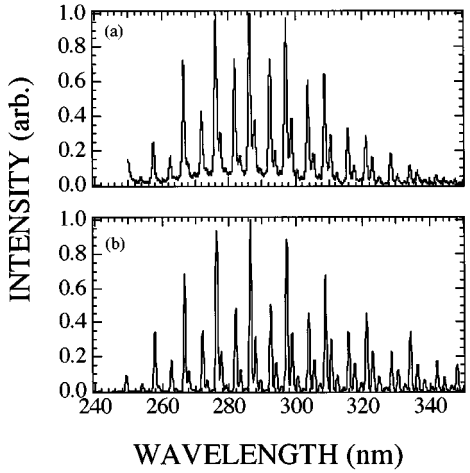

FIG. 2. DF spectrum of NO_2 $\tilde{D}\ ^2B_2(0,0,0)$ in the region of 250–350 nm. (a) Experimental spectrum. (b) Calculated spectrum for the $\tilde{D}\ ^2B_2(0,0,0)\rightarrow\tilde{X}\ ^2A_1(n_1,n_2,n_3)$ transition using reported molecular parameters of $\tilde{D}\ ^2B_2$ and $\tilde{X}\ ^2A_1$ states; $r=131.4$ pm and $\theta=120.8°$ for the $\tilde{D}$ state, $r=119.4$ pm and $\theta=133.9°$ for the $\tilde{X}$ state.

$\omega_1=1244\ cm^{-1}$, $\omega_2=549\ cm^{-1}$, and $\omega_3=365\ cm^{-1}$.[6] Morino *et al.* determined the geometry of NO_2 $\tilde{X}\ ^2A_1(0,0,0)$ to be $r(N–O)=119.4$ pm and $\theta=133.9°$ from the rotational structure of $\tilde{X}\ ^2A_1(0,0,0)$.[11] The vibrational frequencies of $\tilde{X}\ ^2A_1$ were reported by Delon *et al.* as $\omega_1=1347.53\ cm^{-1}$, $\omega_2=758.636\ cm^{-1}$, and $\omega_3=1669.02\ cm^{-1}$.[10] Using these molecular parameters, the Franck–Condon factors of $\tilde{D}\ ^2B_2(0,0,0)\rightarrow\tilde{X}\ ^2A_1(n_1,n_2,0)$ are calculated by the method reported by Coon *et al.*[12] Figure 2(b) shows the simulated spectrum of $\tilde{D}\ ^2B_2(0,0,0)\rightarrow\tilde{X}\ ^2A_1(n_1,n_2,0)$ using the calculated Franck–Condon factors. The simulation reasonably reproduces the fluorescence intensity envelope observed in Fig. 2(a).

B. $\tilde{D}\ ^2B_2(0,0,0)\rightarrow{}^{ev}B_2$ transition

Figure 3 shows the DF spectrum in 350–410 nm, where the Franck–Condon factors of $\tilde{D}\ ^2B_2\rightarrow\tilde{X}\ ^2A_1$ are negligible

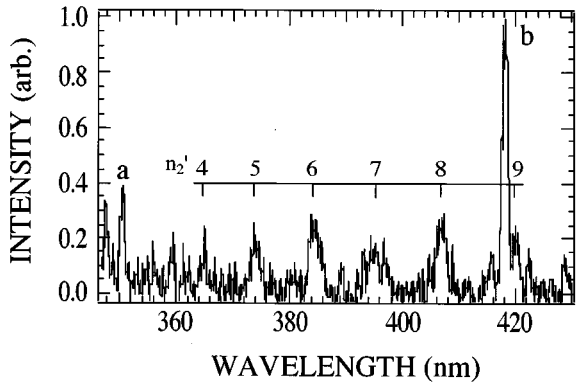

FIG. 3. DF spectrum of NO_2 $\tilde{D}\ ^2B_2(0,0,0)$ in the region of 350–410 nm. Two peaks indicated by ''a'' and ''b'' are assigned to $\tilde{D}\ ^2B_2(0,0,0)\rightarrow\tilde{X}\ ^2A_1(8,2,0)$ and $\tilde{D}\ ^2B_2(0,0,0)\rightarrow\tilde{C}\ ^2A_2(0,0,0)$, respectively.

and only one peak (indicated by ''peak a'' in Fig. 3) could be assigned to the $\tilde{D}\rightarrow\tilde{X}$ transition, $\tilde{D}\ ^2B_2(0,0,0)-\tilde{X}\ ^2A_1(8,2,0)$. One recognizes a weak and broad progression built on the spacing ($\sim$710 cm^{-1}) comparable to the bending frequencies (730–857 cm^{-1}) calculated for $\tilde{A}\ ^2B_2$.[13,14] OODR experiments have been carried out to analyze the rotational structures of the 613 and 674 nm absorption bands,[15,16] the upper vibronic levels of which are located in the same energy regions as the lower vibronic levels of the 420 and 396 nm emission bands, respectively, of Fig. 3. These visible excited states have been confirmed to be of B_2 vibronic symmetry from the OODR experiments.

It is well known that $\tilde{A}\ ^2B_2$ is heavily perturbed by high-lying vibrational levels on $\tilde{X}\ ^2A_1$ through various perturbations, which yields an irregular and dense vibronic manifold of B_2 symmetry ($^{ev}B_2$). The vibronic coupling promoted by antisymmetric stretching vibration is most prominent, and the electronic wave functions of the visible excited states have character of both $\tilde{A}\ ^2B_2$ and $\tilde{X}\ ^2A_1$. It is thus impossible to obtain experimental information on the geometry of NO_2 $\tilde{A}\ ^2B_2$.

Gillispie *et al.*[13] calculated the geometry of $\tilde{A}\ ^2B_2$ as $r(N–O)=126$ pm and $\theta=102°$. More recently, Burton *et al.*[14] have calculated the geometry as 128.1 pm and 101.3°, and the vibrational frequencies as $\omega_1=1391\ cm^{-1}$, $\omega_2=730\ cm^{-1}$, and $\omega_3=359\ cm^{-1}$. Based on these values and the molecular parameters of $\tilde{D}\ ^2B_2$ ($r=131$ pm, $\theta=120.9°$),[6] the $\tilde{D}\ ^2B_2(0,0,0)\rightarrow\tilde{A}\ ^2B_2(n_1,n_2,n_3)$ spectrum is expected to be mainly built on the bending progression, which is in accordance with our observation. We assign the 350–410 nm bands (Fig. 3) to $\tilde{D}\ ^2B_2(0,0,0)\rightarrow{}^{ev}B_2$. The fluorescence intensity seems abnormally low as recognized in Fig. 1, although the $B_2–B_2$ transition is symmetry allowed. This observation is explained by considering the electron configurations of the $\tilde{D}$ and $\tilde{A}$ states. The dominant electron configurations[13] of $\tilde{D}\ ^2B_2$ and $\tilde{A}\ ^2B_2$ are expressed as $\cdots(1a_2)(4b_2)^2(6a_1)(2b_1)$ and $\cdots(1a_2)^2(4b_2)(6a_1)^2$, respectively. Therefore, the $\tilde{D}\ ^2B_2–\tilde{A}\ ^2B_2$ transition is a two-electron transition process and is not expected to be strong. As a result, the intensity of the 350–410 nm bands is at least 10^2 times weaker than that of the 250–350 nm bands. Delon *et al.*[10] reported that the T_0 value of $\tilde{A}\ ^2B_2$ is 9737 cm^{-1}. Using the calculated vibrational frequency ($\omega_2=730$ cm^{-1}), the tentative vibrational assignment can be given as $(0,n_2',0)$ shown in Fig. 3. Since a level with a_1-vibrational symmetry on $\tilde{A}\ ^2B_2$ mixes strongly with a manifold of dense levels with b_2- vibrational symmetry on $\tilde{X}\ ^2A_1$, each emission band will be the superposition of many transition bands terminating on $^{ev}B_2$. Actually, the widths of the $\tilde{D}\rightarrow{}^{ev}B_2$ bands are about two times larger than those of peak a ($\tilde{D}\rightarrow\tilde{X}$) and ''peak b'' ($\tilde{D}\rightarrow\tilde{C}$) as recognized in Fig. 3.

C. $\tilde{D}\ ^2B_2(0,0,0)\rightarrow\tilde{C}\ ^2A_2(n_1,n_2,n_3)$ transition

Figure 1 clearly shows that a new band system starts with a 418.2 nm band, which is regularly followed by a main series of 431.8, 445.9, and 461.0 nm bands. The visible portion of the DF spectrum of $\tilde{D}\ ^2B_2(0,0,0)$ is expanded in Fig.

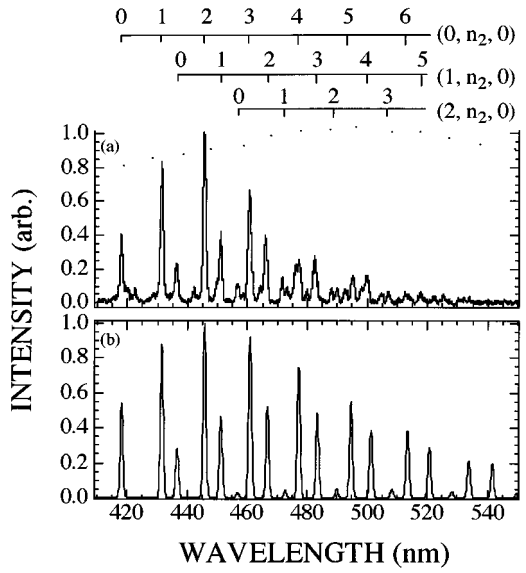

FIG. 4. DF spectrum of NO_2 $\widetilde{D}\ ^2B_2(0,0,0)$ in the region of 410–550 nm. (a) Experimental spectrum. The spectral sensitivity estimated for the grating–photomultiplier combination is shown by dots. (b) Calculated spectrum for $\widetilde{D}\ ^2B_2(0,0,0)\rightarrow\widetilde{C}\ ^2A_2(n_1,n_2,0)$ assuming that the $\widetilde{C}\ ^2A_2$ state has the molecular geometry of $r=133.6$ pm and $\theta=107.9°$.

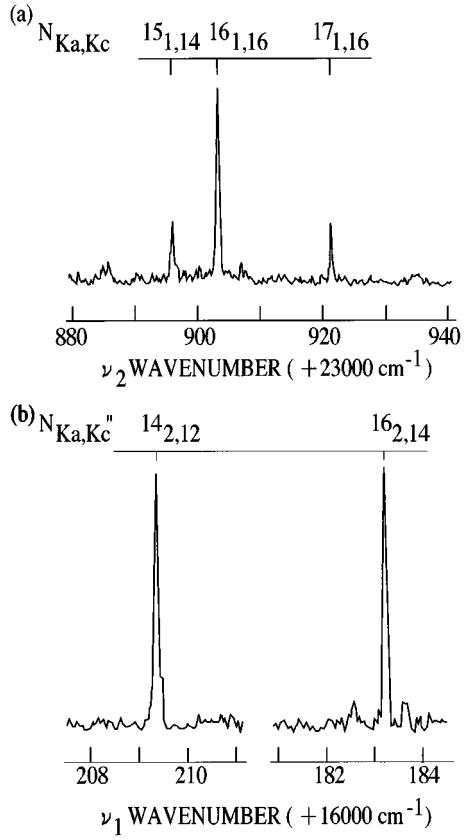

FIG. 5. (a) ν_2-scanned OODR spectrum measured by fixing ν_1 at 16 209.32 cm^{-1}. The same spectrum was obtained by fixing ν_1 at 16 183.08 cm^{-1}. (b) ν_1-scanned spectrum measured by fixing ν_2 at 29 303.0 cm^{-1}.

4(a). Among these bands, the 431.8, 445.9, and 482.7 nm bands have been confirmed to be $\widetilde{D}\ ^2B_2\rightarrow\widetilde{C}\ ^2A_2$ transitions by OODR experiments.[2–4] Many rovibronic levels on $\widetilde{C}\ ^2A_2$ are perturbed by quasicontinum levels on $^{ev}B_2$ (the vibronic state density of $^{ev}B_2\sim13$ cm in the 16 500–18 500 cm^{-1} absorption region)[17] through spin–orbit interaction, and make a number of admixtures of $\widetilde{C}\ ^2A_2/^{ev}B_2$. The OODR excitation via these $\widetilde{C}\ ^2A_2/^{ev}B_2$ admixtures provides us with information on vibronic symmetry of the intermediate states. As a result, the second excitation step in OODR has been concluded to be the $\widetilde{D}\ ^2B_2\leftarrow\widetilde{C}\ ^2A_2$ absorption, which is a reverse process of the $\widetilde{D}\ ^2B_2\rightarrow\widetilde{C}\ ^2A_2$ emission measured in the present experiment. Recently, we have extended OODR experiments to other spectral regions and concluded that the bands at 418.2, 436.7, 451.4, and 461.0 nm are also assigned to $\widetilde{D}\ ^2B_2\rightarrow\widetilde{C}\ ^2A_2$.[16] The energy shifts of rovibronic levels on $\widetilde{C}\ ^2A_2$ are expected to be small, because the spin–orbit interaction between $^2B_2$ and $^2A_2$ vibronic levels is weak.[18] In fact, we have observed energy shifts of less than several cm^{-1}. It is therefore concluded that the progression recognized in Fig. 4(a) essentially reflects the vibrational structure of $\widetilde{C}\ ^2A_2$.

There are some reasons why the $\widetilde{D}\ ^2B_2\rightarrow\widetilde{C}\ ^2A_2$ fluorescence could be measured clearly in the present experiment. (1) The $\widetilde{D}\rightarrow\widetilde{C}$ transition is symmetry allowed and a one electron transition process $(2b_1\rightarrow4a_1)$. It should be mentioned here that the $\widetilde{C}$ state, which is dark from the $\widetilde{X}$ state, becomes light from the $\widetilde{D}$ state. (2) The $\widetilde{D}\ ^2B_2\rightarrow\widetilde{A}\ ^2B_2$ transition is negligibly weak (Fig. 3), because it is a two electron proces $(2b_1\rightarrow4a_1,\ 3b_2\rightarrow1a_2)$. (3) The $\widetilde{D}\ ^2B_2\rightarrow\widetilde{B}\ ^2B_1$ transition $(4a_1\rightarrow1a_2)$ is symmetry forbidden, although the $\widetilde{B}$ state is located at only 0.2 eV below $\widetilde{C}\ ^2A_2$.[19] (4) The $\widetilde{D}\ ^2B_2\rightarrow\widetilde{X}\ ^2A_1$ transition $(2b_1\rightarrow1a_2)$ is negligibly weak in the spectral region (>410 nm) where the $\widetilde{D}\rightarrow\widetilde{C}$ fluorescence is observed.

IV. OPTICAL–OPTICAL DOUBLE RESONANCE

A vibronic level belonging to $\widetilde{C}\ ^2A_2$, which is prepared by the $\widetilde{D}\ ^2B_2(0,0,0)\rightarrow\widetilde{C}$ emission at 418.2 nm (Fig. 4) and which we call ''level A'' is located in the same energy region as the upper vibronic levels prepared by the 617–619 nm absorption of NO_2 $\widetilde{X}\ ^2A_1(0,0,0)$. One can apply an OODR technique to the rotational analysis of level A, if some rotational levels belonging to level A couple through spin–orbit interaction with the quasicontinuum rotational levels on $^{ev}B_2$.[2–4] The rotational structure provides direct information on the vibronic symmetry of a state of interest. We tuned the ν_1 and ν_2 frequencies to 16 160–16 250 cm^{-1} and 23 850–23 950 cm^{-1}, respectively. Typical OODR spectra are shown in Figs. 5(a) and 5(b). The ν_2-scanned spectrum shown in Fig. 5(a) was measured by setting ν_1 at one of the two peaks (16 209.32 and 16 183.08 cm^{-1}) measured in Fig. 5(b) and scanning ν_2 over 23 880–23 950 cm^{-1}. Figure 5(b) shows the ν_1-scanned spectrum, where the ν_2 value was fixed at 23 903.0 cm^{-1}. The rotational quantum numbers determined from the ν_1 and ν_2 transitions are denoted as $N'_{K_a,K_c}(\nu_1)$ and $N'_{K_a,K_c}(\nu_2)$, respectively. The ν_2 transition is a perpendicular band of $\Delta K_a=\pm1$ and terminating on the $15_{1,14}$, $16_{1,16}$, and $17_{1,16}$ levels on $\widetilde{D}\ ^2B_2(0,0,0)$. The interme-

TABLE I. OODR transitions and assignments for $K'_a(\nu_2)=0$ stack measured in the ν_1 region of 16 160–16 220 cm^{-1}.[a]

$D\ ^2B_2(0,0,0)$			Intermediate level					$X\ ^2A_1(0,0,0)$	
$N_{Ka,Kc}$	E_f (cm^{-1})	ν_2 (cm^{-1})	$E_t-\nu_2$	$N'_{Ka,Kc}(\nu_2)$	$N'_{Ka,Kc}(\nu_1)$	$E_i+\nu_1$	ν_1 (cm^{-1})	E_i (cm^{-1})	$N''_{Ka,Kc}$
$3_{1,2}\ F_1$	40 134.3	23 891.8	16 242.5			16 242.33	16 203.69	38.64	$4_{2,2}\ F_2$
$4_{1,4}\ F_1$	40 137.1	23 894.6	16 242.5	$4_{0,4}\ F_1$	$5_{2,3}\ F_2$	16 242.34	16 194.38	47.96	$6_{2,4}\ F_2$
$5_{1,4}\ F_1$	40 141.4	23 898.9	16 242.5						
$4_{1,4}\ F_1$	40 137.1	23 889.8	16 247.3						
$5_{1,4}\ F_1$	40 141.4	23 894.1	16 247.3	$6_{0,6}F_1$	$6_{2,5}F_1$	16 247.32	16 204.33	42.99	$5_{2,4}\ F_1$
$6_{1,6}\ F_1$	40 145.3	23 897.8	16 247.3			16 247.30	16 193.35	53.95	$7_{2,6}\ F_1$
$7_{1,6}\ F_1$	40 151.6	23 904.3	16 247.3						
$7_{1,6}\ F_1$	40 151.6	23 884.4	16 267.2			16 267.32	16 206.67	60.65	$8_{2,6}\ F_2$
$8_{1,8}\ F_1$	40 156.6	23 889.3	16 267.3	$8_{0,8}\ F_1$	$9_{2,7}\ F_2$				
$9_{1,8}\ F_1$	40 165.0	23 897.6	16 267.4			16 267.31	16 190.60	76.71	$10_{2,8}\ F_2$
						16 262.27	16 215.86	46.41	$10_{0,10}\ F_2$
$9_{1,8}\ F_1$	40 165.0	23 902.6	16 262.4		$11_{0,11}\ F_2$	16 262.25	16 196.46	65.79	$12_{0,12}\ F_2$
$10_{1,10}\ F_1$	40 170.8	23 908.5	16 262.3	$10_{0,10}\ F_1$					
$11_{1,10}\ F_1$	40 181.5	23 919.3	16 262.2			16 262.25	16 185.54	76.71	$10_{2,8}\ F_2$
					$11_{2,9}\ F_2$	16 262.25	16 166.10	96.15	$10_{2,10}\ F_2$
$13_{1,12}\ F_1$	40 201.1	23 898.0	16 303.1			16 303.35	16 214.81	88.54	$14_{0,14}\ F_2$
$14_{1,14}\ F_1$	40 208.2	23 904.9	16 303.3	$14_{0,14}\ F_1$	$15_{0,15}\ F_2$				
$15_{1,14}\ F_1$	40 223.9	23 920.7	16 303.2			16 303.37	16 188.74	114.63	$16_{0,16}\ F_2$
$15_{1,14}\ F_2$	40 223.9	23 895.0	16 328.9			16 328.77	16 209.76	119.01	$14_{2,12}\ F_1$
$16_{1,16}\ F_2$	40 231.4	23 902.5	16 328.9	$16_{0,16}\ F_2$	$15_{2,13}\ F_1$				
$17_{1,16}\ F_2$	40 249.7	23 920.9	16 328.8			16 328.75	16 183.08	145.23	$16_{2,14}\ F_1$
$15_{1,14}\ F_2$	40 223.9	23 895.5	16 328.4			16 328.39	16 209.38	119.01	$14_{2,12}\ F_1$
$16_{1,16}\ F_2$	40 231.4	23 903.0	16 328.4	$16_{0,16}\ F_2$	$15_{2,13}\ F_1$				
$17_{1,16}\ F_2$	40 249.7	23 921.4	16 328.3			16 328.40	16 183.17	145.23	$16_{2,14}\ F_1$

[a]Rotational quantum numbers of an intermediate state independently determined by ν_2 and ν_1 transitions are indicated by $N'_{Ka,Kc}(\nu_2)$ and $N'_{Ka,Kc}(\nu_1)$, respectively. Two electron spin fine components ($J=N+1/2$ and $J=N-1/2$) are denoted by F_1 and F_2, respectively. The rovibronic energy (E_{evr}) is calculated by ($E_i+\nu_1$) and ($E_f-\nu_2$) with accuracies of 0.04 and 0.3 cm^{-1}, respectively.

diate rotational level is thus assigned as $N'_{K_a,K_c}(\nu_2) = 16_{0.16}$ from the ν_2 scanned spectrum [Fig. 5(a)]. Using the rotational constants for $\tilde{X}\ ^2A_1(0,0,0)$,[9] the two lines in Fig. 5(b) are assigned to the ν_1 transitions of a parallel type ($\Delta K_a=0$) originating from the $14_{2.12}$ and $16_{2.14}$ levels on $\tilde{X}\ ^2A_1(0,0,0)$. The quantum number of the intermediate level is thus determined as $N'_{K_a,K_c}(\nu_1) = 15_{2.13}$ from the ν_1-scanned spectrum [Fig. 5(b)]. Table I lists all the ν_1 and ν_2 transitions and assignments for the $K'_a(\nu_2) = 0$ levels detected by the OODR method in the ν_1 region of 16 160–16 220 cm^{-1} (617–619 nm). All of the intermediate levels have even $N'(\nu_2)$. Figure 6 plots the rovibronic energies against $N'(\nu_2)[N'(\nu_2)+1]$.

Nitrogen dioxide belongs to a C_{2v} point group. According to nuclear statistics, the rovibronic symmetry of NO_2 is restricted to A symmetry species ($^{evr}A_1$ or $^{evr}A_2$). Therefore, the $B(^{ev}B_1$ or $^{ev}B_2)$ and $A(^{ev}A_1$ or $^{ev}A_2)$ vibronic states have only the rotational levels with odd and even N quantum numbers, respectively, in the $K_a=0$ stack. All the intermediate rovibronic levels with $K'_a(\nu_2) = 0$ are found to have even $N'(\nu_2)$ as shown in Table I, which implies that the intermediate levels are on $^{ev}A_1$ or $^{ev}A_2$. The ν_2 transition is either a parallel type of $^{ev}B_2 \leftarrow {}^{ev}A_1$ or a perpendicular type of $^{ev}B_2 \leftarrow {}^{ev}A_2$. The experiment shows that the ν_2 transition is perpendicular as recognized in Fig. 5(a). The ν_2 transition is assigned definitely to $^{ev}B_2 \leftarrow {}^{ev}A_2$.

The upper states of the visible absorption of NO_2 $\tilde{X}\ ^2A_1$ are dominantly of $^{ev}B_2$ symmetry, where the $^{ev}B_2$ states are generated by strong vibronic interaction between a_1 vibra-

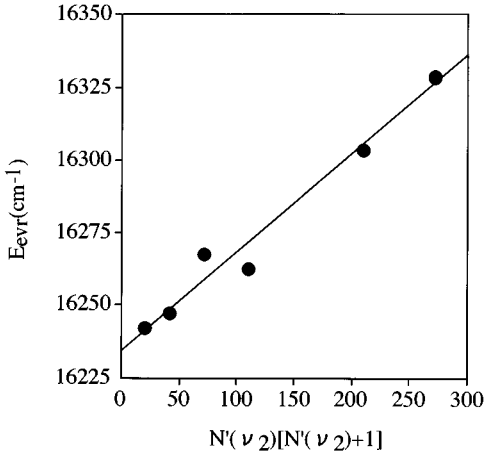

FIG. 6. Plot of rovibronic energies for $K'_a(\nu_2) = 0$ stack, E_{evr}, against $N'(\nu_2)[N'(\nu_2)+1]$. The data are taken from Table I.

tional levels on $\tilde{A}\ ^2B_2$ and b_2-vibrational levels on the ground state. Accordingly, the intermediate rovibronic levels (level A), which are prepared by the 617–619 nm absorption of NO_2 $\tilde{X}\ ^2A_1$ and detected by the present OODR method, are admixture states of $^{ev}B_2$ and $^{ev}A_2$ symmetry.

There are two candidates for the $^{ev}A_2$ state detected by the ν_2 transitions in OODR; a_1- vibrational levels on $\tilde{C}\ ^2A_2$ and b_2-vibrational levels on $\tilde{B}\ ^2B_1$. The possibility of the latter case is excluded, since the $\tilde{D}\ ^2B_2$–$\tilde{B}\ ^2B_1$ transition is symmetry forbidden and the $\tilde{D}\ ^2B_2 \leftarrow \tilde{B}\ ^2B_1$ transition is Franck–Condon forbidden in this energy region.[4] Therefore, the rovibronic levels (level A) observed in these OODR experiments are concluded to belong to a certain a_1 vibrational level on $\tilde{C}\ ^2A_2$.

V. VIBRATIONAL STRUCTURE OF $\tilde{C}\ ^2A_2$

From the OODR experiment (Table I), the smallest ν_1 frequency to prepare $^{ev}A_2$ is determined to be 16 166 cm^{-1} (λ_1~619 nm), which corresponds to the ν_2 frequencies of 23 902–23 919 cm^{-1} (λ_2~418 nm). The ν_2 frequencies of 23 902–23 919 cm^{-1} are in accord with the largest frequency of 23 800±17 cm^{-1}(418.2±0.3 nm) among the $\tilde{D}\ ^2B_2 \rightarrow \tilde{C}\ ^2A_2$ bands [Fig. 4(a)]. Thus, the $\tilde{D}\ ^2B_2(0,0,0)$ emission band at 418.2 nm is assigned to $\tilde{D}^2B_2(0,0,0) \rightarrow \tilde{C}\ ^2A_2(0,0,0)$. In other words, level A is concluded to be $\tilde{C}\ ^2A_2(0,0,0)$.

The T_0 value of $\tilde{C}\ ^2A_2$ is determined to be around 16 234 cm^{-1} from the rotational energy structure of $\tilde{C}\ ^2A_2(0,0,0)$ shown in Fig. 6. The T_0 value of $\tilde{C}\ ^2A_2$ is also estimated from the DF spectrum (Fig. 4). The $14_{2.13}$ level on $\tilde{D}\ ^2B_2(0,0,0)$ with E_{evr}=40 221.4 cm^{-1} is mainly generated with the photoexcitation of NO_2 at 249.29 nm. The $\tilde{D}\ ^2B_2(0,0,0) \rightarrow \tilde{C}\ ^2A_2(0,0,0)$ transition at 418.2±0.3 nm prepares the rotational levels on $\tilde{C}\ ^2A_2(0,0,0)$ with E_{evr}=16310±20 cm^{-1}. These levels contain the averaged rotational energy of about 90 cm^{-1}, which is estimated using the rotational constants of A=2.8 cm^{-1} and B=0.4 cm^{-1}. The resultant T_0 value is 16 220±20 cm^{-1}, which agrees with the T_0 value of 16 234 cm^{-1} determined from the OODR analysis. Weaver *et al.*[1] reported the T_0 value of 16 360±70 cm^{-1} from their photoelectron spectrum of NO_2^-. Their value does not agree with the T_0 value obtained in the present work. There exist many $^{ev}B_2$ states near $\tilde{C}\ ^2A_2(0,0,0)$. Actually, only the $^{ev}B_2$ levels were observed in the absorption region of 612–614 nm (16 287–16 341 cm^{-1}).[15] The origin of the $\tilde{C}\ ^2A_2$ state determined by photoelectron spectroscopy seems to be not as accurate due to the overlapping problem.

Gillispie *et al.* calculated the bending frequency (ω_2) of $\tilde{C}\ ^2A_2$ to be 798 cm^{-1} at a multiconfiguration self-consistent-field (MCSCF) level.[13] Burton *et al.* reported the calculated frequencies as 882 cm^{-1} at a SCF level and 828 cm^{-1} at a complete-active-space self-consistent-field (CASSCF) level.[14] The terminating level corresponding to the DF band at 431.8 nm of NO_2 $\tilde{D}\ ^2B_2(0,0,0)$ lies at 750 cm^{-1} above $\tilde{C}\ ^2A_2(0,0,0)$. The energy separation almost agrees with the bending frequency predicted by the theoretical calculations. Accordingly, the DF band at 431.8 nm is assigned to $\tilde{D}\ ^2B_2(0,0,0) \rightarrow \tilde{C}\ ^2A_2(0,1,0)$.

The ω_1 value is calculated to be 1360 cm^{-1} by Gillispie *et al.*[13] The terminating level of the DF band at 436.7 nm lies at 1010 cm^{-1} above $\tilde{C}\ ^2A_2(0,0,0)$. This band is thus assigned to $\tilde{D}\ ^2B_2(0,0,0) \rightarrow \tilde{C}\ ^2A_2(1,0,0)$.

Katagiri and Kato[20] have reported that the potential surface of $\tilde{C}\ ^2A_2$ along the asymmetric vibrational coordinate (the $1\ ^2A''$ state) correlates to the limit of $NO(^2\Pi)+O(^3P)$ dissociation. The dissociation limit lies at about 3 eV above $\tilde{X}\ ^2A_1(0,0,0)$, and the A''-potential depth is only about 1 eV. Burton *et al.*[14] calculated the ω_3 value of $\tilde{C}\ ^2A_2$ to be as small as 227 cm^{-1} at the CASSCF level. B_1-vibronic levels with odd n_3 on $\tilde{C}\ ^2A_2$ cannot be the terminating ones of the $\tilde{D} \rightarrow \tilde{C}$ emission, because the $^{ev}B_2$–$^{ev}B_1$ transition is symmetry forbidden. However, rotational levels on $^{ev}B_1$ ($^{ev}A_2 \times {}^{v}b_2$) are perturbed by near-lying rotational levels on $^{ev}B_2$ and $^{ev}A_1$ through spin–orbit interaction to generate admixture states of $^{ev}B_2/^{ev}B_1$ and $^{ev}A_1/^{ev}B_1$.[17] The perturbation may break vibronic symmetry, which permits us to observe the B_2–B_1 forbidden transition. Delon *et al.* reported similar examples:[10] Many symmetry-forbidden bands terminating on the b_2-vibrational levels on $\tilde{X}\ ^2A_1$ were observed in the DF spectrum of $^{ev}B_2 \rightarrow \tilde{X}\ ^2A_1$. It is reasonable that the $\tilde{D}\ ^2B_2(0,0,0) \rightarrow {}^{ev}B_2/^{ev}B_1$ bands have a transition intensity comparable to the $\tilde{D}\ ^2B_2(0,0,0) \rightarrow {}^{ev}B_2$ ($n_2' = 4-9$) bands shown in Fig. 4. The terminating level corresponding to a weak DF band at 422.6 nm of $\tilde{D}\ ^2B_2(0,0,0)$ lies at 250 cm^{-1} above $\tilde{C}\ ^2A_2(0,0,0)$. We tentatively assign this weak band at 422.6 nm to $\tilde{D}\ ^2B_2(0,0,0) \rightarrow \tilde{C}\ ^2A_2(0,0,1)$.

The main vibrational assignments of the DF bands are shown in Fig. 4(a). The detailed vibrational assignments and vibronic term values of $\tilde{C}\ ^2A_2$ are listed in Table II. Due to a relation that $\omega_1=\omega_2+\omega_3$, several bands are assigned to two vibrational levels of $\tilde{C}\ ^2A_2$; $(n_1,n_2,0)/(n_1-1,n_2+1,1)$. In the DF experiments, $\tilde{D}\ ^2B_2(0,0,0) \rightarrow \tilde{C}\ ^2A_2(n_1,n_2,0)$ will have major contributions in intensity.

The intensity patterns of the $\tilde{D} \rightarrow \tilde{C}$ flourescence seems abnormal in the region longer than 470 nm. Jackels and Davidson[21] calculated the electronic potential surfaces of NO_2 and found that $\tilde{C}\ ^2A_2$ and $\tilde{B}\ ^2B_1$ intersect each other around 17 100 cm^{-1} above $\tilde{X}\ ^2A_1(0,0,0)$ at the bond angle close to the equilibrium one in the ground state. The vibronic mixing between $\tilde{C}\ ^2A_2$ and $\tilde{B}\ ^2B_1$ through antisymmetric vibration may be responsible for the abnormal intensity pattern.

VI. GEOMETRY OF $\tilde{C}\ ^2A_2$

The Franck–Condon analysis of the DF spectrum of $\tilde{D}\ ^2B_2(0,0,0) \rightarrow \tilde{C}\ ^2A_2(n_1,n_2,n_3)$ gives the geometry difference between $\tilde{C}\ ^2A_2$ and $\tilde{D}\ ^2B_2$. The intensity pattern in the region shorter than 470 nm was used for the Franck–Condon fitting. The electronic transition moment was assumed to be constant over the range of interest. The Franck–Condon maximum occurs at $\Delta n_1=0$ and $\Delta n_2=2$. The C_{2v} symmetry of the $\tilde{C}$ and $\tilde{D}$ states was also assumed and therefore the $\Delta n_3=1$ transition does not appear in simulation. The DF

TABLE II. Summary of the vibrational structure of NO_2 $\widetilde{C}\ ^2A_2$ obtained from DF and OODR experiments.

DF experiment			OODR experiment		Assignment
λ_{em} (nm)[a]	E_{evr} (cm^{-1})[b]	E_v (cm^{-1})[c]	E_{ev} (cm^{-1})[d]	E_v (cm^{-1})[e]	(n_1,n_2,n_3)
418.2	16 310	0	16 234	0	(0,0,0)
422.6	16 560	250			(0,0,1)
431.8	17 060	750	16 970[f]	736	(0,1,0)
436.7	17 320	1010	17 230[g]	996	(1,0,0)/(0,1,1)
442.5	17 620	1310			(1,0,1)
445.9	17 790	1480	17 709[h]	1475	(0,2,0)
450.0	18 000	1690			(0,2,1)
451.4	18 070	1760	17 974[g]	1740	(1,1,0)
456.9	18 330	2020	18 255[g]	2021	(2,0,0)/(1,1,1)
461.0	18 530	2220	18 455[g]	2221	(0,3,0)
466.3	18 780	2470			(1,2,0)/(0,3,1)
471.8	19 030	2720			(1,2,1)
473.5	19 100	2790			(2,1,0)
476.4	19 230	2920			(2,1,1)?
477.2	19 270	2960			(0,4,0)
480.1	19 390	3080			(3,0,0)
482.7	19 500	3190	19 499[i]	3215	(1,3,0)/(0,4,1)
488.4	19 750	3440			(1,3,1)
490.2	19 830	3520			(2,2,0)
493.0	19 940	3630			(2,2,1)?
495.3	20 030	3720			(0,5,0)
500.0	20 220	3910			(1,4,0)
505.0	20 420	4110			(1,4,1)?
507.1	20 500	4190			(2,3,0)?
512.7	20 720	4410			(0,6,0)?

[a]Single photon excitation near the $^qR_2$ bandhead of the $\widetilde{D}\ ^2B_2 \leftarrow \widetilde{X}\ ^2A_1(0,0,0)$ transition (40 113.9 cm^{-1}).
[b]Rovibronic energies (E_{evr}) determined by subtracting the emission energies from the excitation energy. They contain rotational energies of about 90 cm^{-1} (see the text).
[c]Vibrational energies (E_v) determined by the relation $E_v = E_{ev} - 16\,310$ cm^{-1}.
[d]Vibronic energies (E_{ev}) determined by OODR experiments. For example, the value for $\widetilde{C}\ ^2A_2(0,0,0)$ was obtained from a linear approximation of the plots in Fig. 6.
[e]Vibrational energies (E_v) determined by the relation $E_v = E_{ev} - 16\,234$ cm^{-1}.
[f]Data taken from Ref. 3.
[g]Data taken from Ref. 16.
[h]Data taken from Ref. 4.
[i]Data taken from Ref. 2.

spectrum of $\widetilde{D} \rightarrow \widetilde{C}$ could be reasonably simulated under the conditions that $\Delta r = 2$–3 pm and $\Delta\theta = -(12$–$13°)$. The spectrum simulated for $\Delta r = 2.2$ pm and $\Delta\theta = -13°$ is shown in Fig. 4(b). The $\widetilde{D}\ ^2B_2$ geometry is reported as r(N–O)=131.4 pm and $\theta = 120.9°$.[6] Accordingly, from the equilibrium geometry of NO_2 $\widetilde{C}\ ^2A_2$ it is concluded that r(N–O)=133.4–134.4 pm and $\theta = 107.9°$–$108.9°$.

Table III lists the geometric parameters of $\widetilde{C}\ ^2A_2$ ob-

TABLE III. Summary of the geometric parameters of NO_2 $\widetilde{C}\ ^2A_2$ obtained by experiments and calculations.

	Experiment					Calculation		
	Franck–Condon analysis		Rotational analysis					
	This work	PES[a]	(0,2,0)[b]	(2,0,0)[c]	(1,3,0)[d]	MCSCF[e]	CASSCF[f]	SCF[g]
r (pm)	133.9±1.0	⋯	134	141	140	127	126.2	123.5
ω (deg)	108.4±1.0	<110	109	103	102	110	109.8	109.9

[a]Photoelectron spectroscopy, Ref. 1.
[b]Data are taken from Ref. 4.
[c]Data are taken from Ref. 16.
[d]Data are taken from Ref. 2.
[e]Multiconfiguration self-consistent field method, Ref. 13.
[f]Complete-active-space self-consistent field method, Ref. 14.
[g]Self-consistent field method, Ref. 14.

tained by experiments and calculations. The $\tilde{C}\ ^2A_2$ geometry obtained in this study almost agrees with the other experimental and theoretical values. Weaver *et al.*[1] estimated the bond angle of NO_2 $\tilde{C}\ ^2A_2$ to be smaller than 110°, based on their photoelectron spectrum of NO_2.[1] The theoretical calculations report that r(N–O)=123.5–127 pm and θ=109.8–110°. The bend structure of $\tilde{C}\ ^2A_2$ comes from the dominant electron configuration expressed as $\cdots(1a_2)(4b_2)^2(6a_1)^2$. Among the molecular orbitals of XY_2-type molecules, the $6a_1$ orbital is known to be most sensitive to the bond angle ($\angle YXY$), and prefers strongly the rectangular structure rather than the linear. Thus, the equilibrium bond angle of NO_2 is primarily controlled by the number of electrons occupied by the $6a_1$ orbital as follows:

$(6a_1)^2$ configuration

$$\cdots(1a_2)(4b_2)^2(6a_1)^2:\ \tilde{C}\ ^2A_2,\quad \theta=109°$$

$$\cdots(1a_2)^2(4b_2)(6a_1)^2:\ \tilde{A}\ ^2B_2,\quad \theta=102°$$

$(6a_1)^1$ configuration

$$\cdots(1a_2)(4b_2)^2(6a_1)(2b_1):\ \tilde{D}\ ^2B_2,\quad \theta=131°$$

$$\cdots(1a_2)^2(4b_2)^2(6a_1):\ \tilde{X}\ ^2A_1,\quad \theta=134°$$

$(6a_1)^0$ configuration

$$\cdots(1a_2)^2(4b_2)(2b_1):\ \tilde{B}\ ^2B_1(^2\Pi),\quad \theta=180°$$

The geometric parameters also depend on the vibronic states as seen in Table III. The variation of the molecular parameters may originate from the distortion of the rotational structure due to perturbation and/or vibrational effect.

ACKNOWLEDGMENTS

The authors are grateful to Professor Kinichi Obi for his encouragement throughout this work. The authors wish to express their thanks to Junichi Oike and Kiyoshi Nakata for helping us in a part of the experiments. This work was partly supported by Sumitomo Foundation.

[1] A. Weaver, R. B. Metz, S. E. Bradforth, and D. M. Neumark, J. Chem. Phys. **90**, 2070 (1989).
[2] K. Shibuya, T. Kusumoto, H. Nagai, and K. Obi, J. Chem. Phys. **95**, 720 (1991).
[3] H. Nagai, K. Aoki, T. Kusumoto, K. Shibuya, and K. Obi, J. Phys. Chem. **95**, 2718 (1991).
[4] K. Aoki, H. Nagai, K. Hoshina, and K. Shibuya, J. Phys. Chem. **97**, 8889 (1993).
[5] K. Tsukiyama, K. Shibuya, K. Obi, and I. Tanaka, J. Chem. Phys. **82**, 1147 (1985).
[6] K.-E. J. Hallin and A. J. Merer, Can. J. Phys. **54**, 1157 (1976).
[7] I. B. Berlman, *Handbook of Fluorescence Spectra of Aromatic Molecules* (Academic, New York, 1971).
[8] K. Shibuya, T. Kusumoto, H. Nagai, and K. Obi, Chem. Phys. Lett. **152**, 129 (1988).
[9] W. Bowman and F. C. DeLucia, J. Chem. Phys. **77**, 92 (1982).
[10] A. Delon and R. Jost, J. Chem. Phys. **95**, 5686 (1991).
[11] Y. Morino, M. Tanimoto, S. Saito, and E. Hirota, J. Mol. Spectrosc. **98**, 331 (1983).
[12] J. B. Coon, R. E. Dewames, and C. M. Loyd, J. Mol. Spectrosc. **8**, 285 (1962).
[13] G. D. Gillispie, A. U. Khan, A. C. Wahl, R. P. Hostney, and M. Krauss, J. Chem. Phys. **63**, 3425 (1975).
[14] N. A. Burton, Y. Yamaguchi, I. L. Alberts, and H. F. Shaefer III, J. Chem. Phys. **95**, 7466 (1991).
[15] H. Nagai, K. Shibuya, and K. Obi, J. Chem. Phys. **93**, 7656 (1990).
[16] K. Shibuya, K. Hoshina, K. Nakata, and K. Aoki (unpublished).
[17] A. Delon, R. Jost, and M. Lombardi, J. Chem. Phys. **95**, 5701 (1991); R. Georges, A. Delon, and R. Jost, *ibid*. **103**, 1732 (1995).
[18] K.-E. J. Hallin and A. J. Merer, Can. J. Phys. **65**, 163 (1977).
[19] J. L. Hardwick and J. C. D. Brand, Chem. Phys. Lett. **21**, 458 (1973).
[20] H. Katagiri and S. Kato, J. Chem. Phys. **99**, 8805 (1993).
[21] C. F. Jackels and E. R. Davidson, J. Chem. Phys. **65**, 2941 (1976).